Journal of High Energy Physics, Gravitation and Cosmology, 2026, 12(2), 935-944
https://www.scirp.org/journal/jhepgc
ISSN Online: 2380-4335
ISSN Print: 2380-4327

Cosmic Filaments without Dark Matter: Cylindrical Vacuum Localized Structures as Exact Relativistic Solutions

Rudi Van Nieuwenhove

Independent Researcher, Dessel, Belgium
Email: rvnieuwe@gmail.com

How to cite this paper: Van Nieuwenhove, R. (2026) Cosmic Filaments without Dark Matter: Cylindrical Vacuum Localized Structures as Exact Relativistic Solutions. *Journal of High Energy Physics, Gravitation and Cosmology*, **12**, 935-944.
https://doi.org/10.4236/jhepgc.2026.122051

Received: January 16, 2026
Accepted: April 4, 2026
Published: April 7, 2026

Copyright © 2026 by author(s) and Scientific Research Publishing Inc.
This work is licensed under the Creative Commons Attribution International License (CC BY 4.0).
http://creativecommons.org/licenses/by/4.0/

Open Access

Abstract

Cosmic filaments constitute one of the most prominent components of the large-scale structure of the Universe, forming coherent, elongated bridges between clusters and superclusters of galaxies. In the standard cosmological framework, these structures are interpreted as dark-matter-dominated density enhancements produced by the gravitational amplification of primordial fluctuations. In this work, we explore an alternative description based on Vacuum Localized Structures (VLS): self-gravitating solutions of the Einstein field equations characterized by a non-standard vacuum equation of state. We derive and analyze a new class of exact, cylindrically symmetric VLS solutions of the Einstein equations, appropriate to modelling extended filamentary systems. These solutions are supported by an effective stress-energy tensor with radial pressure $p_r = -\rho/3$, generalising the equation of state previously identified in spherical VLS configurations. We characterise the resulting spacetime, study its gravitational field, and show that it naturally gives rise to coherent, non-singular, extended structures with finite mass per unit length. The present cylindrical solutions extend earlier work on spherical VLS, where galactic-scale configurations were shown to reproduce key features of observed rotation curves without invoking particle dark matter. Taken together, the spherical and cylindrical solutions provide a unified relativistic framework in which both galactic halos and cosmic filaments emerge as manifestations of vacuum-organized gravitational structures. We discuss the physical properties of cylindrical VLS, their potential stability, and their relevance to observed filament phenomenology, including coherence length, mass distribution, and large-scale dynamical effects. These results suggest that vacuum localized structures may offer a viable alternative foundation for the gravitational scaffolding of the cosmic web.

Keywords

Cosmic Filaments, General Relativity, Cosmology, Dark Matter Alternatives

1. Introduction

Observations from large spectroscopic galaxy redshift surveys reveal that galaxies are not randomly distributed but are arranged in an intricate network of nodes, walls, voids, and filamentary structures extending across cosmological scales. Deep redshift surveys like the Sloan Digital Sky Survey (SDSS) enable three-dimensional mapping of the galaxy distribution, with filamentary structures identified systematically in these data and characterized using persistent structure extraction algorithms [1]. These cosmic filaments span tens to hundreds of megaparsecs and connect dense clusters of galaxies, forming the backbone of the so-called cosmic web. Filaments often contain a significant fraction of the galaxy population and contribute substantially to the observed large-scale structure of the universe [2].

The environment within filaments appears to influence galaxy properties: galaxies located closer to filament axes tend to be more massive, show suppressed star formation compared to counterparts in the field, and exhibit morphological differences consistent with environmental processing [3].

Beyond the galaxy distribution, intergalactic gas associated with filaments has been detected through indirect means, such as X-ray observations and statistical signatures in cosmic microwave background studies (e.g., via the Sunyaev-Zel'dovich effect), lending support to the notion that filaments host a warm-hot intergalactic medium (WHIM) that may harbour a significant portion of the universe's "missing" baryons [4].

Recent high-sensitivity radio observations have even revealed coherent dynamical signatures in filaments. In a rare case, a massive filamentary structure several tens of megaparsecs long exhibits rotational motion, with galaxies on opposite sides of the filament moving in opposite directions, implying coherent motion on an unprecedented scale [5].

Together, these observational results establish several robust empirical characteristics of cosmic filaments: they are coherent, elongated structures traced by galaxies and gas; they influence the properties of galaxies embedded within them; they contain diffuse baryonic matter; and, in exceptional cases, they show evidence of large-scale kinematic coherence.

Large-scale galaxy surveys and cosmological N-body simulations consistently reveal a striking network of clusters, walls, voids, and filaments known as the cosmic web. Within the standard ΛCDM framework, these filamentary structures are commonly interpreted as the natural outcome of gravitational amplification of primordial density fluctuations. However, despite their prominence, the physical origin of extended filaments has not been scrutinized in detail. Recent analyses

have raised the possibility that a non-negligible fraction of these large-scale filamentary patterns may not be genuine predictions of an initially isotropic cosmological model, but instead reflect subtle anisotropies introduced at the level of numerical initial conditions [6]. In particular, it has been shown that the widely used procedure of generating initial conditions by applying correlated displacements to a regular cubic lattice unavoidably imprints directional correlations that are invisible to standard, angle-averaged diagnostics, yet persist and are amplified by gravitational evolution. These residual anisotropies can seed filamentary features that survive into the linear and mildly non-linear regimes, calling into question whether all simulated large-scale filaments truly originate from primordial density correlations. This opens the door to reasonable doubt regarding the standard interpretation of filament formation and motivates the exploration of alternative physical mechanisms capable of producing coherent, filamentary cosmic structures.

Besides MOND, another recently proposed alternative to dark matter is the concept of Vacuum Localized Structures (VLS) [7] [8]. These objects are solutions of the standard Einstein field equations and are characterized by a radial pressure equal to minus one third of the energy density. VLS can in principle exist on a wide range of scales and, when extended to galactic dimensions, have been shown to reproduce galaxy rotation curves without invoking dark matter. For this framework to also account for the large-scale scaffolding of the cosmic web, it is necessary that cylindrical VLS solutions exist which can play the same dynamical role as dark matter in the standard picture of filament formation. In this paper, we demonstrate that such solutions to the Einstein field equations indeed exist, thereby completing the conceptual extension of vacuum localized structures from galactic systems to the filamentary backbone of the Universe.

2. Einstein Field Equations in Cylindrical Geometry

We start from the static, cylindrically symmetric metric in tangential gauge

$$\mathrm{d}s^2 = -\mathrm{e}^{2\Phi(r)}\mathrm{d}t^2 + \mathrm{e}^{2\Lambda(r)}\mathrm{d}r^2 + r^2\mathrm{d}\phi^2 + \mathrm{e}^{2\Psi(r)}\mathrm{d}z^2. \tag{1}$$

The Einstein equations and conservation law are taken from [9], in particular Equations (34)-(38) and Equation (41).

$$0 = p_r' + p_r\left(\Phi' + \Psi' + \frac{1}{r}\right) + \rho\Phi' - p_z\Psi' - \frac{1}{r}p_\phi \tag{2}$$

$$4\pi\left(\rho + p_r + p_\phi + p_z\right)\mathrm{e}^{2\Lambda} = \Phi'' + \Phi'^2 - \Phi'\Lambda' + \Psi'\Phi' + \frac{1}{r}\Phi' \tag{3}$$

$$4\pi\left(\rho + p_r - p_\phi - p_z\right)\mathrm{e}^{2\Lambda} = -\Phi'' - \Phi'^2 + \Phi'\Lambda' + \frac{1}{r}\Lambda' - \Psi'' - \Psi'^2 + \Lambda'\Psi' \tag{4}$$

$$4\pi\left(\rho - p_r + p_\phi - p_z\right)\mathrm{e}^{2\Lambda} = \frac{1}{r}\left(\Lambda' - \Phi' - \Psi'\right) \tag{5}$$

$$4\pi\left(\rho - p_r - p_\phi + p_z\right)\mathrm{e}^{2\Lambda} = -\Psi'' - \Psi'^2 + \Psi'\Lambda' - \Psi'\Phi' - \frac{1}{r}\Psi' \tag{6}$$

$$8\pi p_r e^{2\Lambda} = \Phi'\Psi' + \frac{1}{r}(\Phi' + \Psi'). \tag{7}$$

Using the weak-field approximation, we assume that

$$|\Phi|, |\Psi|, |\Lambda| \ll 1, \tag{8}$$

and neglect all quadratic derivative terms. Also,

$$e^{2\Lambda} \simeq 1. \tag{9}$$

The linearized equations become

$$0 = p_r' + p_r\left(\Phi' + \Psi' + \frac{1}{r}\right) + \rho\Phi' - p_z\Psi' - \frac{1}{r}p_\phi \tag{10}$$

$$\Phi'' + 1/r\,\Phi' = 4\pi(\rho + p_r + p_\phi + p_z), \tag{11}$$

$$-\Phi'' + \tfrac{1}{r}\Lambda' - \Psi'' = 4\pi(\rho + p_r - p_\phi - p_z) \tag{12}$$

$$\frac{1}{r}(\Lambda' - \Phi' - \Psi') = 4\pi(\rho - p_r + p_\phi - p_z) \tag{13}$$

$$-\Psi'' - \frac{\Psi'}{r} = 4\pi(\rho - p_r - p_\phi + p_z) \tag{14}$$

$$\Phi' + \Psi' = 8\pi p_r r. \tag{15}$$

3. Stress-Energy Tensor

Next, we impose our matter model as;

$$p_r = -\frac{1}{3}\rho, \quad p_z = 0, \tag{16}$$

and take a Gaussian density profile

$$\rho(r) = \rho_0 e^{-r^2/R^2}. \tag{17}$$

Negative pressure is often associated with repulsive gravity, especially in cosmological contexts. However, within localized gravitational systems, negative pressure does not in itself imply repulsion or instability. What governs the gravitational behaviour is the full relativistic balance encoded in the Einstein equations and, for static configurations, in the generalized Tolman-Oppenheimer-Volkoff equilibrium condition, which allows for anisotropic stresses and admits configurations with negative radial pressure when appropriately balanced by geometry and transverse stresses.

Indeed, a variety of well-known relativistic solutions demonstrate that negative pressure can play a constructive structural role. Gravastar models, for example, employ vacuum-like negative pressure regions to support non-singular, self-gravitating objects. Traversable wormhole geometries similarly require negative radial pressure (or tension) to maintain their throats, and under suitable conditions can be dynamically stable. On cosmological scales, de Sitter space itself provides a maximally symmetric and stable solution of Einstein's equations supported entirely by negative pressure.

These examples illustrate that negative pressure is not inherently pathological, but can act as an organizing agent for equilibrium space-time structures. In the present context, the specific value $p_r = -\rho/3$ emerges as the condition that permits coherent, non-singular, extended vacuum configurations without introducing repulsive large-scale behaviour. It therefore represents a physically admissible and geometrically motivated equation of state for vacuum localised structures, suitable for constructing both spherical and cylindrical gravitational systems.

Trendafilova and Fulling [9] demonstrated that the general class of static, cylindrically symmetric vacuum solutions is unavoidably singular on the symmetry axis and must therefore be supplemented by interior matter models, including the special case $\rho = -p_z$, $p_r = p_\phi = 0$, corresponding to cosmic-string-type sources.

The present work differs fundamentally in that the cylindrical VLS constitutes a globally regular solution of the Einstein equations with a non-string equation of state, remaining finite at $r = 0$ and describing a self-contained filamentary configuration rather than a vacuum exterior matched to an ad-hoc interior.

The appearance of a non-standard vacuum equation of state raises the question of how such a stress-energy content should be physically interpreted. In contemporary quantum field theory, the vacuum is not treated as a material medium, but rather as the ground state of interacting quantum fields, characterised by correlations, fluctuations, and symmetry properties. While this framework successfully accounts for microscopic phenomena, it does not provide a macroscopic description of the vacuum as a continuum with effective mechanical or elastic properties. General relativity, however, couples only to the coarse-grained stress-energy tensor, independently of the microscopic origin of that structure.

From this perspective, the equation of state $p_r = -\rho/3$ may be viewed as a phenomenological description of an organised vacuum configuration, encoding how the vacuum responds to self-consistent gravitational structuring. Rather than representing a fluid of particles, it characterises an effective vacuum stiffness or tension associated with spatial organisation. In this sense, vacuum localised structures may be interpreted as emergent geometric states of the vacuum, whose large-scale gravitational behaviour admits a continuum description even in the absence of a complete microscopic theory.

4. Solution

The azimuthal pressure $p_\phi(r)$ is not imposed.
Combining Equation (15) and Equation (10), we obtain

$$p_\phi = -\frac{1}{3} r\rho' - \frac{1}{3}\rho. \tag{18}$$

With the Gaussian profile,

$$p_\phi(r) = -\frac{\rho}{3}\left(1 - 2\frac{r^2}{R^2}\right) = p_r\left(1 - 2\frac{r^2}{R^2}\right) \tag{19}$$

The equation for Φ becomes

$$\Phi'' + \frac{1}{r}\Phi' = \frac{4\pi}{3}\rho\left(1 + \frac{2r^2}{R^2}\right). \tag{20}$$

Equivalently,

$$\left(r\Phi'\right)' = \frac{4\pi\rho_0}{3}\left(r + \frac{2r^3}{R^2}\right)\mathrm{e}^{-r^2/R^2}. \tag{21}$$

The regular solution is obtained by integrating from 0 to r:

$$r\Phi'(r) = \frac{4\pi\rho_0}{3}\int_0^r \left(s + \frac{2s^3}{R^2}\right)\mathrm{e}^{-s^2/R^2}\mathrm{d}s. \tag{22}$$

This gives

$$\Phi'(r) = \frac{2\pi\rho_0 R^2}{r}\left(1 - \mathrm{e}^{-r^2/R^2}\right) - \frac{4\pi\rho_0}{3} r\mathrm{e}^{-r^2/R^2}. \tag{23}$$

The weak-field gravitational force per unit mass is

$$g(r) = -\Phi'(r). \tag{24}$$

Thus

$$g(r) = -2\pi\rho_0 R^2 \frac{1 - \mathrm{e}^{-r^2/R^2}}{r} + \frac{4\pi\rho_0}{3} r\mathrm{e}^{-r^2/R^2}. \tag{25}$$

The force vanishes linearly at the axis and the geometry is regular.
From Equation (15), $\Psi'(r)$ follows.

$$\Psi' = -\frac{2\pi\rho_0 R^2}{r}\left(1 - \mathrm{e}^{-\frac{r^2}{R^2}}\right) - \frac{4\pi\rho_0 r\mathrm{e}^{-\frac{r^2}{R^2}}}{3} \tag{26}$$

It can be verified that this equation is consistent with Equation (14).
From combining the linearized Einstein Equations (13) and (15) one obtains Λ':

$$\Lambda' = \Phi' + \Psi' + 4\pi r\left(\frac{4}{3}\rho + p_\phi\right). \tag{27}$$

This yields

$$\Lambda' = \frac{4\pi}{3}\rho r + \frac{8\pi}{3}\frac{r^3}{R^2}\rho. \tag{28}$$

Integrating,

$$\Lambda(r) = 2\pi\rho_0 R^2\left[1 - \mathrm{e}^{-r^2/R^2}\left(1 + \frac{2r^2}{3R^2}\right)\right]. \tag{29}$$

Further, it is useful to obtain an equation for the mass of the cylindrical solution per unit of length (μ). Integrating the density profile yields:

$$\mu = \pi\rho_0 R^2 \tag{30}$$

A weak-field cylindrical VLS core with $p_r = -\rho/3$ and Gaussian density admits a fully analytic, regular interior solution. The azimuthal pressure is dynamically generated and the force vanishes linearly at the axis. The solution provides a con-

sistent analytic seed for cylindrical VLS modeling and matching to an exterior Weyl-Levi-Civita vacuum.

Define $x = r/R$. Then

$$\begin{aligned}
&\rho(x) = \rho_0 \mathrm{e}^{-x^2}, \\
&p_\phi(x) = \rho_0 \mathrm{e}^{-x^2}\left(\frac{2x^2}{3} - \frac{1}{3}\right), \\
&\rho_{\text{Tolman}}(x) = \rho + p_r + p_\phi = \rho_0 \mathrm{e}^{-x^2}\left(\frac{1}{3} + \frac{2x^2}{3}\right), \\
&g(x) = -2\pi\rho_0 R\left[\frac{1-\mathrm{e}^{-x^2}}{x} - \frac{2}{3}x\mathrm{e}^{-x^2}\right], \\
&\Lambda(x) = 2\pi\rho_0 R^2\left[1 - \mathrm{e}^{-x^2}\left(1 + \frac{2x^2}{3}\right)\right].
\end{aligned} \tag{31}$$

Plots of densities, pressures and the inward acceleration are shown in Figures 1-3.

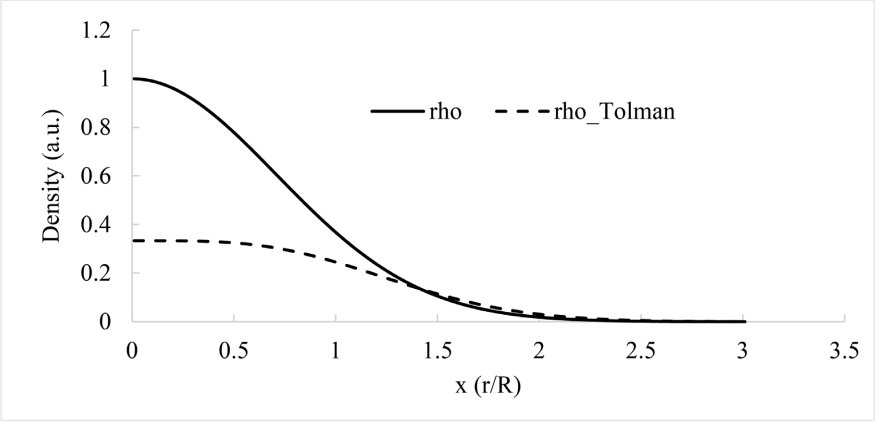

Figure 1. Profiles of normalized density (rho) and Tolman density (rho_Tolman).

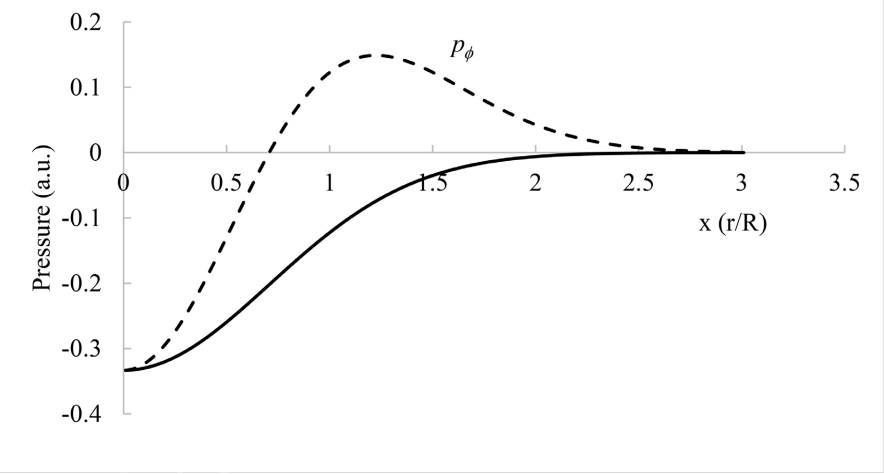

Figure 2. Profiles of normalized radial (p_r) and azimuthal (p_ϕ) pressures.

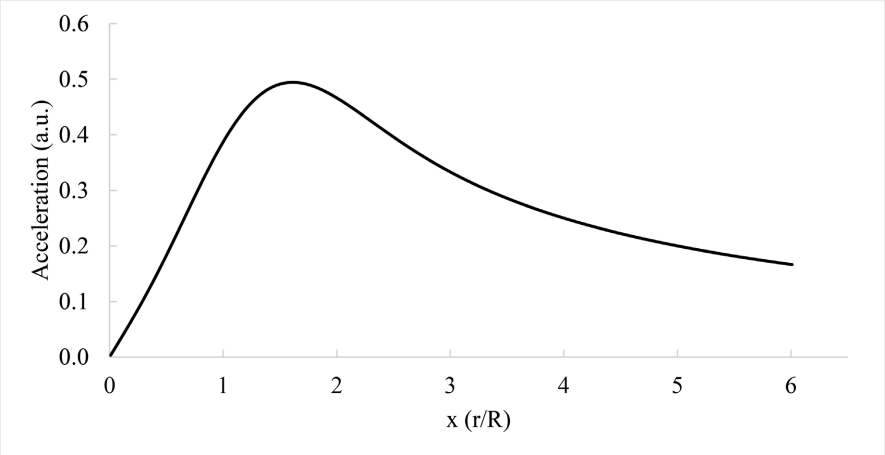

Figure 3. Radial profile of the normalized acceleration. The acceleration is inward (towards $x = 0$).

5. Application to a Filament

Weak gravitational lensing and multiwavelength observations provide direct empirical constraints on the physical scale of cosmic filaments, although current detections usually probe only limited filament segments, most commonly intercluster or inter-galaxy bridges. Stacked weak-lensing analyses of luminous red galaxy pairs find an excess mass of order $10^{13} M_{\odot}$ distributed over bridge regions ~7 - 10 h^{-1} Mpc long and ~2 - 3h^{-1} Mpc wide, implying characteristic filament radii of order $R \sim 1$ - 2 Mpc (≈3 × 10^{22} - 6 × 10^{22} m) and typical line-masses $\Lambda \sim 10^{12}$ - $10^{13} M_{\odot}$ Mpc^{-1} (≈10^{20} - 10^{21} kg·m^{-1}) for the prominent filament population [10]. Individual detections of intercluster filaments, such as the Abell 222/223 system, extend over comparable or larger projected distances ($\gtrsim 10$ Mpc) and confirm the presence of coherent dark-matter structures connecting massive nodes [11]. These observed bridge lengths reflect the scale over which filaments can be cleanly isolated in data and should not be interpreted as the full extent of cosmic filaments, which in large-scale galaxy surveys and cosmic-web reconstructions frequently trace continuous, curved structures spanning many tens of megaparsecs, implying intrinsic aspect ratios $L/R \gg 10$.

There is currently no consensus on a universal radial density profile for cosmic filaments. Observational constraints from stacked weak-lensing and galaxy-density measurements indicate smooth, centrally enhanced profiles with shallow radial gradients and no sharp boundary, but do not uniquely distinguish between cored power-law, exponential, or Gaussian-type forms.

For a Gaussian filament profile $\rho(r) = \rho_0 e^{-r^2/R^2}$ with $R = 4 \times 10^{22}$ m and $\mu = 5.0 \times 10^{20}$ kg·m^{-1}, the implied central density $\rho_0 = \mu / (\pi R^2) \simeq 1 \times 10^{-25}$ kg·m^{-3}, corresponding to a central overdensity of $\rho_0 / \bar{\rho}_m \sim 30$ - 40 relative to the present cosmic mean matter density $\bar{\rho}_m \simeq 3 \times 10^{-27}$ kg·m^{-3}, well within the range inferred observationally for prominent cosmic filaments. To obtain the acceleration in units of m/s^2, one has to multiply the normalized acceleration (see **Figure 3**) by the factor $2\pi R \rho_0 G = 1.68 \times 10^{-12}$ m/s^2.

6. Summary

Cosmic filaments are among the most striking and least understood components of the large-scale structure of the Universe. While they are routinely reproduced in cosmological simulations and interpreted within the dark-matter paradigm as density enhancements arising from gravitational instability, their physical nature and degree of inevitability within standard assumptions remain open to question. This work has been motivated by the possibility that at least part of the filamentary cosmic network may reflect an underlying class of coherent gravitational structures rather than merely the late-time arrangement of collisionless matter.

In this paper, we have constructed and analysed a new class of exact, cylindrically symmetric solutions of the Einstein field equations describing *Vacuum Localized Structures*. These solutions are characterised by an effective stress-energy content with radial equation of state $p_r = -\rho/3$, extending the vacuum localized structure concept from spherical to filamentary geometries. The resulting spacetimes are non-singular, spatially extended, and possess a finite mass per unit length, making them natural relativistic candidates for modelling cosmic filaments.

The central novelty of the present work lies in the explicit demonstration that the Einstein equations admit self-consistent cylindrical VLS configurations. This establishes, for the first time, that vacuum localized structures are not restricted to isolated, approximately spherical systems, but can also exist as coherent, elongated gravitational entities. Together with earlier spherical VLS solutions that account for galactic rotation curves without invoking dark matter, the cylindrical solutions presented here complete a minimal geometric set of vacuum structures capable of reproducing both galactic and filamentary components of the cosmic web.

Beyond providing a new exact solution, this work opens a broader conceptual perspective in which the gravitational scaffolding of the Universe may be interpreted as arising from organised vacuum configurations rather than from an unseen matter component. The existence of cylindrical VLS suggests new avenues for investigating filament stability, interactions between filaments and galaxies, and possible observational discriminants between vacuum-structured and particle-dark-matter descriptions. These directions will be explored in future work.

Conflicts of Interest

The author declares no conflicts of interest regarding the publication of this paper.

References

[1] Tempel, E., Stoica, R.S., Martínez, V.J., Liivamägi, L.J., Castellan, G. and Saar, E. (2014) Detecting Filamentary Pattern in the Cosmic Web: A Catalogue of Filaments for the SDSS. *Monthly Notices of the Royal Astronomical Society*, **438**, 3465-3482. https://doi.org/10.1093/mnras/stt2454

[2] Malavasi, N., Aghanim, N., Douspis, M., Tanimura, H. and Bonjean, V. (2020) Char-

acterizing Filaments in the SDSS Volume from the Galaxy Distribution. *Astronomy & Astrophysics*, **642**, A19. https://doi.org/10.1051/0004-6361/202037647

[3] O'Kane, C.J., Kuchner, U., Gray, M.E. and Aragón-Salamanca, A. (2024) The Effect of Cosmic Web Filaments on Galaxy Evolution. *Monthly Notices of the Royal Astronomical Society*, **534**, 1682-1699. https://doi.org/10.1093/mnras/stae2142

[4] Eckert, D., Jauzac, M., Shan, H., Kneib, J., Erben, T., Israel, H., *et al.* (2015) Warm-Hot Baryons Comprise 5-10 Per Cent of Filaments in the Cosmic Web. *Nature*, **528**, 105-107. https://doi.org/10.1038/nature16058

[5] Tudorache, M.N., Jung, S.L., Jarvis, M.J., Heywood, I., Ponomareva, A.A., Vărăşteanu, A.A., *et al.* (2025) A 15 Mpc Rotating Galaxy Filament at Redshift $Z = 0.032$. *Monthly Notices of the Royal Astronomical Society*, **544**, 4306-4316. https://doi.org/10.1093/mnras/staf2005

[6] Sylos Labini, F. (2026) Hidden Role of Anisotropies in Shaping Structure Formation in Cosmological N-Body Simulations. *Physical Review D*, **113**, Article 023510. https://doi.org/10.1103/5jtj-tbs5

[7] Van Nieuwenhove, R. (2025) Galactic Geons: Revisiting the Dark Matter Paradigm, Fund. *Journal of Modern Physics*, **23**, 1-16.

[8] Van Nieuwenhove, R. (2025) Galaxy Rotation Curves from Self-Consistent Gravitational Energy Distributions. *Proceedings of XI Meeting on Fundamental Cosmology*, Santander, 18-20 November 2025.

[9] Trendafilova, C.S. and Fulling, S.A. (2011) Static Solutions of Einstein's Equations with Cylindrical Symmetry. *European Journal of Physics*, **32**, 1663-1677. https://doi.org/10.1088/0143-0807/32/6/020

[10] Epps, S.D. and Hudson, M.J. (2017) The Weak-Lensing Masses of Filaments between Luminous Red Galaxies. *Monthly Notices of the Royal Astronomical Society*, **468**, 2605-2613. https://doi.org/10.1093/mnras/stx517

[11] Dietrich, J.P., Werner, N., Clowe, D., Finoguenov, A., Kitching, T., Miller, L., *et al.* (2012) A Filament of Dark Matter between Two Clusters of Galaxies. *Nature*, **487**, 202-204. https://doi.org/10.1038/nature11224